

Synthesis of microsphere aluminum hypophosphite and its application in polyurethane elastomer

Wen-Zong Xu,^{1,2} Peng-Cheng Wang,¹ Shao-Qing Wang,¹ Yuan Hu²

¹School of Materials Science and Chemical Engineering, Anhui Jianzhu University, 292 Ziyun Road, Hefei 230601, Anhui Province, People's Republic of China

²State Key Lab of Fire Science, University of Science and Technology of China, Hefei, Anhui 230026, People's Republic of China
Correspondence to: W. Z. Xu (E-mail: wenzongxu@ahjzu.edu.cn)

ABSTRACT: Microsphere aluminum hypophosphite (AHP) is prepared via the hydrothermal method and characterized by Fourier transform infrared spectrometry, X-ray diffraction, and scanning electron microscopy. Then the hydrothermal AHP and the precipitation AHP are added to the polyurethane elastomer (PUE). The flame retardant properties, thermal stability, and mechanical properties of the PUE with different kinds of AHP added are studied. The results show that the hydrothermal AHP is microsphere with a uniform particle size of around 5 μm . The limited oxygen index of the PUE with the addition of 5% hydrothermal AHP increases to 28.5 vol %. Compared with the PUE including different kinds of AHP, the peak heat release rate of added hydrothermal AHP decreases by about 6%. Hydrothermal AHP could improve the char yield which provides better flame retardancy for PUE. Meanwhile, the hydrothermal AHP-added PUE has better mechanical properties than that with precipitation AHP added. © 2015 Wiley Periodicals, Inc. *J. Appl. Polym. Sci.* **2015**, *132*, 42370.

KEYWORDS: flame retardance; polyurethanes; properties and characterization

Received 6 December 2014; accepted 16 April 2015

DOI: 10.1002/app.42370

INTRODUCTION

Aluminum hypophosphite (AHP) is a kind of environmentally friendly halogen-free and nontoxic flame retardant with excellent performance due to its 41.89% phosphorus content, excellent thermal stability, and flame retardant performance.^{1–4} As a new type of flame retardant applied in polymer materials, it has a pretty good effect.^{5–8} The application of AHP prepared by precipitation in polystyrene (PS) was studied by Yuzhong Wang *et al.*,⁹ and their results show that 25 wt % of the AHP could make composites achieve a UL-94 V0 rating with a limited oxygen index (LOI) value of 25.6 vol %, improving the flame retardant performance and reducing the heat release rate of PS composites effectively. Wei Yang *et al.* applied precipitation prepared AHP and montmorillonite together into polybutylene terephthalate (PBT)/glass fiber (GF) composites,¹⁰ and their results showed that 10 wt % of AHP could make composites achieve a UL-94 V0 rating with an LOI value of 28.5 vol %, not only improving the flame retardant properties of the composites, but also reducing its toxic gas production significantly. Bihe Yuan studied the application of AHP in polyvinyl alcohol (PVA), and found that AHP could effectively reduce the heat release rate of PVA and increase char residue,¹¹ and 15 wt % of AHP could make the AHP/PVA composites achieve a UL-94 V0 rating with

an LOI value of 30.0 vol %. However, AHP prepared by the precipitation method has a less satisfactory distribution and dispersion in composites with different particle sizes and morphology.

Polyurethane elastomers possess excellent abrasion resistance, oil resistance, tear resistance, resistance to chemical corrosion, and high elastic properties. However, general polyurethane materials, which are not resistant to combustion, is limited in practical application. Therefore, improving the flame retardancy has received much attention.¹²

In this study, AHP was prepared via the hydrothermal method and characterized by Fourier transform infrared spectrometry (FTIR), X-ray diffraction (XRD), and scanning electron microscopy (SEM). Furthermore, the hydrothermal-prepared AHP and precipitation-prepared AHP were introduced into PUE to investigate the different effects on thermal stability, flame retardancy, and mechanical properties resulting from different kinds of AHP.

EXPERIMENTAL

Materials

Precipitation AHP was purchased from Wuhan Ruiji Chemical Co., Ltd. of China. Sodium hypophosphite was purchased from Tianjin Kemio Chemical Co., Ltd., China. Aluminum chloride,

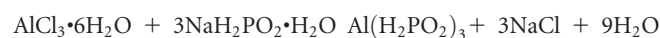
Table I. Description of the PUE and PUE/AHP Composites

Sample	Prepolymer (g)	MOCA (g)	AHP (g)		Content of AHP (wt %)
			Hydrothermal	Precipitation	
PUE	45.31	4.69	0	0	0
AHPPUE1	44.86	4.64	0.5	0	1
AHPPUE2	43.05	4.45	2.5	0	5
AHPPUE3	40.78	4.22	5	0	10
AHPPUE4	44.86	4.64	0	0.5	1
AHPPUE5	43.05	4.45	0	2.5	5
AHPPUE6	40.78	4.22	0	5	10

ethanol, and polyvinylpyrrolidone (PVP K-30) were purchased from Sinopharm Chemical Reagent Co., Ltd., China. Toluene diisocyanate (TDI) was purchased from Mitsui Chemical Co., Ltd., Japan. Polyester diol ($M_n = 1975$) was purchased from Shandong Dexin Chemical Co., Ltd., China. 3,3'-dichloro-4,4'-diaminodiphenylmethane (MOCA) was purchased from Jinan Haiwu Chemical Co., Ltd., China.

Synthesis of Microsphere Aluminum Hypophosphite

In a typical experiment, 0.993 g aluminum chloride ($AlCl_3 \cdot 6H_2O$) was dissolved in 25 mL deionized water with 30 min continuous stirring at room temperature and 2.332 g sodium hypophosphite ($NaH_2PO_2 \cdot H_2O$) was added to this colorless solution. Then, 45 mL ethanol and 1.0 g PVP were added, followed by 30 min stirring. Afterward, these mixtures were independently transferred into Teflon-lined stainless steel autoclaves of 100 mL capacity. The autoclaves were tightly closed and heated at 230°C for 7 h in an electric oven and then cooled down to room temperature naturally. AHP $Al(H_2PO_2)_3$ was synthesized, separated by filtration, washed with distilled water and ethanol, and dried at 80°C in an electric oven for 24 h.



Synthesis of Polyurethane Elastomers

Polyester diol was heated to 110°C, stirred, and vacuumed for 2 h to remove trace water. After that, the vacuuming was stopped. When the temperature was reduced to 75°C, TDI was added and reacted for 2 h; in this way, prepolymer was prepared.

The chain extender, AHP, and prepolymer were mixed and stirred fully. Then, the mixture was casted on a teflon mold at 80°C for 8 h and placed in an oven at 120°C for 4 h. Finally, the polyurethane elastomers were synthesized. Table I presents the description of PUE and AHP-PUEs.

Characterization

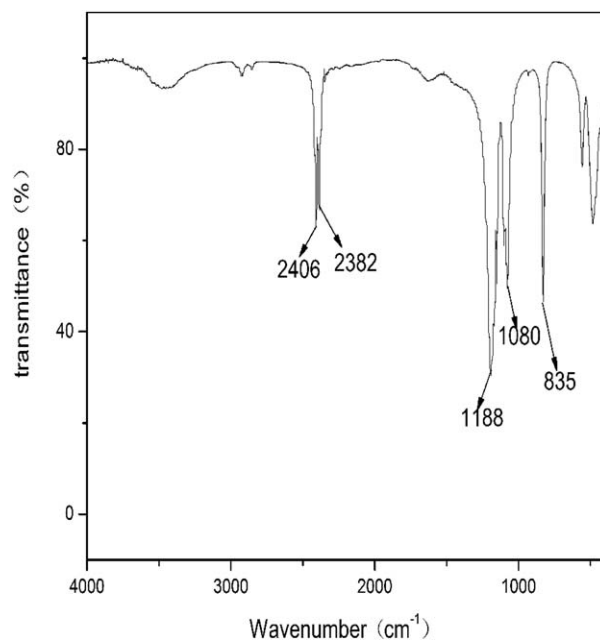
FTIR was obtained with a Nicolet 6700 FT-IR spectrophotometer (Thermo Fisher Scientific, U.S.) using KBr pellets. XRD was obtained with a Bruker D8 ADVANCE diffractometer (BRUKER, Germany), with a scanning rate of 2° min^{-1} and a range of 10–70°. Thermogravimetric analysis (TGA) was carried out on an STA 409PC (NETZSCH, Germany) thermoanalyzer instrument from room temperature to 600°C at a linear heating rate of $20^\circ \text{ C min}^{-1}$ under an N_2 atmosphere. The

weight of all the samples were kept within 5–10 mg. Cone calorimeter combustion tests were performed on a cone calorimeter (Jiangning Analysis Instrument Company, China) according to ISO 5660 standard procedures. Square specimens ($100 \times 100 \times 3 \text{ mm}^3$) were irradiated at a heat flux of $50 \text{ kW} \cdot \text{m}^{-2}$. The LOI was measured using an HC-2 oxygen index meter (Jiangning Analysis Instrument Company, China), according to ASTM D2863. Dimensions of the samples were $100 \times 10 \times 4 \text{ mm}^3$, five samples were tested to obtain average values. SEM was obtained with a JEOL JSM-7500F (JEOL, Japan). The specimens were sputter-coated with a conductive layer. Tensile test results were obtained with a 3010 universal experimental machine (Shenzhen reger Company, China), according to ISO8256-2004, under an extension speed of $300 \text{ mm} \cdot \text{min}^{-1}$ at room temperature. The tensile specimens were dumbbells. Five samples were tested to obtain average values.

RESULTS AND DISCUSSION

Characterization of Hydrothermal Aluminum Hypophosphite

FTIR spectrum of hydrothermal AHP is shown in Figure 1. The peaks at 2408 and 2382 cm^{-1} correspond to PH_2 stretching.

**Figure 1.** FTIR spectrum of hydrothermal aluminum hypophosphite.

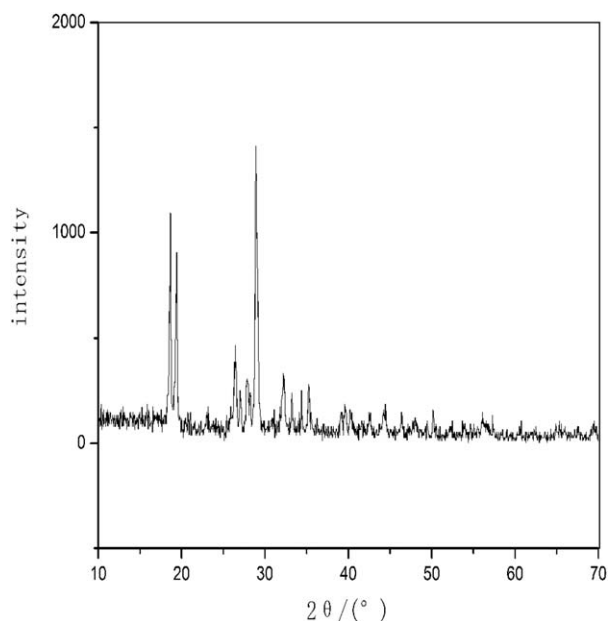


Figure 2. XRD spectrum of hydrothermal aluminum hypophosphite.

The peaks at 1188 cm^{-1} corresponds to $\text{P}=\text{O}$ stretching. The peak at 1140 cm^{-1} is attributed to $\text{P}-\text{O}$ bond. The medium intensity peak at 835 cm^{-1} can be attributed to the rocking mode of PH_2 . These peaks are similar to the literature,¹³ proving that the product is hypophosphite.

XRD spectrum of hydrothermal AHP is shown in Figure 2. There are several main characteristic diffraction peaks at 2θ angles of 18° , 20° , and 29° . These peaks can be well indexed to AHP. No characteristic peaks are observed for other impurities. These peaks are similar to the literature,¹⁴ proving that the product is AHP.

The SEM micrographs of different kinds of AHP are presented in Figure 3. The micrograph (a) shows that the hydrothermal AHP has a spherical morphology, uniform dimension, and a

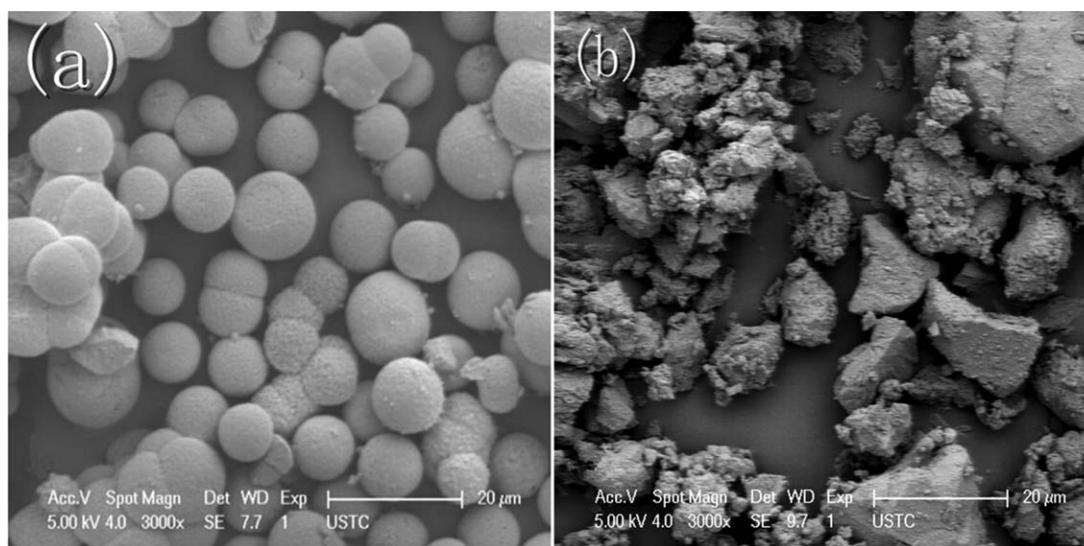


Figure 3. SEM images of different kinds of AHP: (a) hydrothermal aluminum hypophosphite and (b) precipitation aluminum hypophosphite.

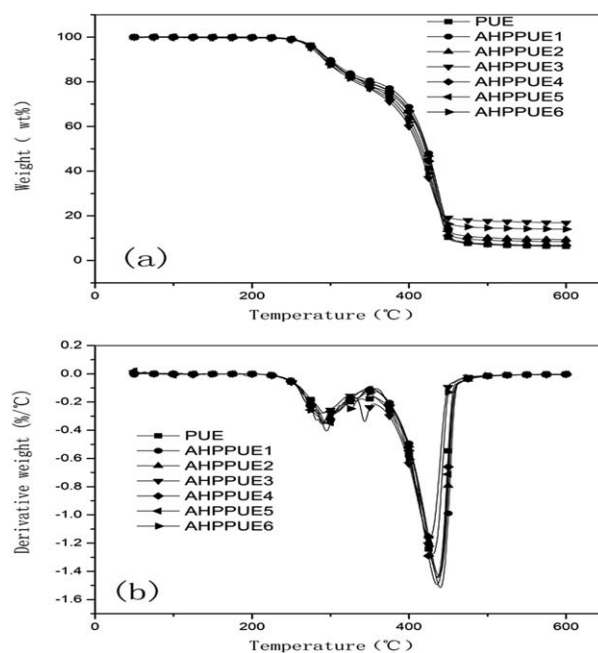


Figure 4. (a) TGA and (b) DTG curves of PUE and PUE/AHP composites.

particle size of about $5\ \mu\text{m}$, while the micrograph (b) shows that the precipitation AHP has different morphologies and sizes from 5 to $20\ \mu\text{m}$.

Thermal Stability Behavior of PUE/AHP Composites

TGA and differential thermogravimetric (DTG) curves of PUE and PUE/AHP composites under nitrogen atmosphere are shown in Figure 4, and the data are summarized in Table II. Obviously, pure PUE decomposition is divided into two stages: the first stage decomposition temperature ranging from 220 to 290°C , and the second stage decomposition temperature ranging from 228 to 414°C . This is because the molecular chain of PUE is composed of hard segment and soft segment, the former

Table II. TG and DTG Data of PUE and PUE/AHP Composites

Sample	T_5 (°C)	T_{50} (°C)	T_{max1} (°C)	T_{max2} (°C)	Residues (wt %)
PUE	281.8	418.2	290.5	436.1	6.3
AHPPUE1	279.5	423.1	290.5	440.2	6.7
AHPPUE2	279.5	422.5	290.5	438.5	9.3
AHPPUE3	275.5	412.8	290.5	426.5	16.8
AHPPUE4	279.5	420.5	290.5	435.5	6.6
AHPPUE5	279.4	420.9	290.5	437.0	8.4
AHPPUE6	276.3	415.3	290.5	430.0	14.0

including aromatic and ureido groups, and the latter including ester, ether, and methylene groups. Compared with these groups, the thermal stability of groups in the hard segment is poorer than that in the soft segment, so the decomposition temperature of hard segment is lower than that of the soft segment. Comparing AHPPUE3 with AHPPUE6, the decomposition temperature as T_5 means the temperature at 5 wt % mass loss, T_{50} means the temperature at 50 wt % mass loss, and T_{max2} means the temperature at the maximum weight loss are similar, which illustrates that these two kinds of AHP have similar effects on the thermal stability. Comparing the carbon residue rate of the PUE, AHPPUE1-3, and AHPPUE4-6, we can find that the char residue is greatly affected by the incorporation of AHP. And the char residue of the PUE with hydrothermal AHP added is higher than that of the PUE with precipitation AHP added.

Cone Calorimetric Analysis of PUE/AHP Composites

At present, the cone calorimeter combustion test is widely used to assess the fire behavior of materials in real accidents.¹⁵ In this study, it was employed to evaluate the flame retardancy of pure PUE and PUE/AHP systems. All the curves of the heat release rate (HRR), total heat release (THR), and mass loss (ML) are presented in Figures 5–7, and their corresponding quantitative data are listed in Table III. For pure PUE, the values of the peak heat release rate (PHRR) and THR are $618.7 \text{ kW} \cdot \text{m}^{-2}$ and $35.3 \text{ MJ} \cdot \text{m}^{-2}$, respectively. With the hydrothermal AHP content increased up to 5 wt %, these values are further decreased. The values are $117.9 \text{ kW} \cdot \text{m}^{-2}$ and $17.7 \text{ MJ} \cdot \text{m}^{-2}$, correspondingly. Compared with pure PUE, the PHRR and THR decrease by 80.1 and 49.8%, respectively. The addition of AHP results in a gradually decreasing trend of PHRR and THR value for PUE/AHP composites with an increase in the AHP loading. The ML of pure PUE is the largest, and the carbon residue is the lowest. The carbon residue of AHP-added PUE is higher than that of pure PUE. In addition, with the increase of AHP, the carbon residue increases significantly; the carbon residue increases by 230% when 10 wt % hydrothermal AHP is added.

In order to investigate the inner structure of the composites, the composites with a hydrothermal AHP and precipitation AHP loading of 10.0 wt % were cryogenically broken after immersion in liquid nitrogen and the fractured surfaces were characterized by SEM (Figure 8). Figure 8(a) shows that hydro-

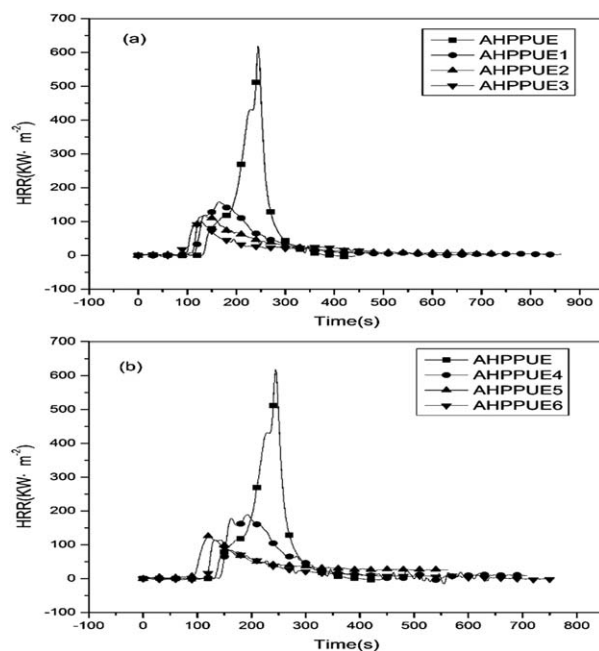


Figure 5. HRR curves of PUE and PUE/AHP composites: (a) PUE with hydrothermal aluminum hypophosphite added and (b) PUE with precipitation aluminum hypophosphite added.

thermal AHP has good interfacial adhesion with PUE matrix in the composite, which exhibits uniformly dispersed morphology. However, precipitation AHP in PUE [Figure 8(b)] matrix has a small amount of agglomeration.

Compared with the data of PUE having the same amount of different types of AHP, we can find that the PUE with hydrothermal AHP added has a lower PHRR and THR rate and

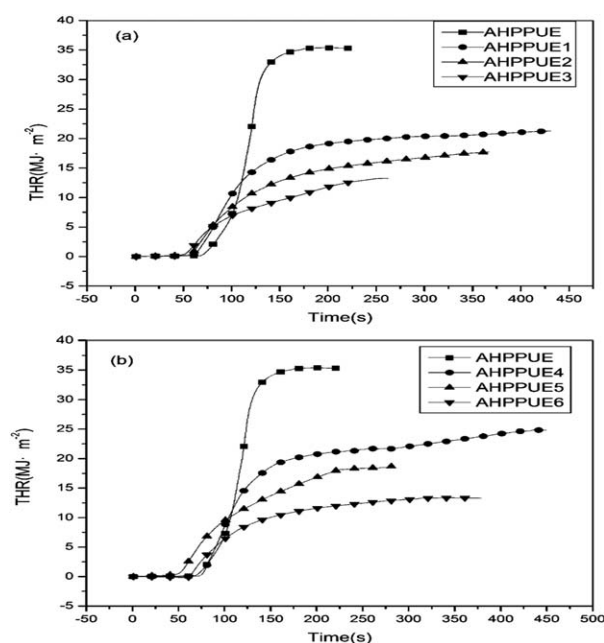


Figure 6. THR curves of PUE and PUE/AHP composites: (a) PUE with hydrothermal aluminum hypophosphite added and (b) PUE with precipitation aluminum hypophosphite added.

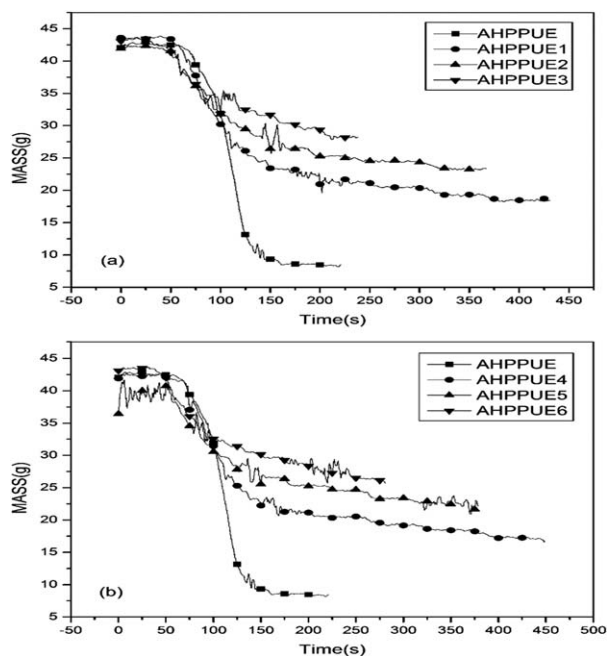


Figure 7. ML curves of PUE and PUE/AHP composites: (a) PUE with hydrothermal aluminum hypophosphite added and (b) PUE with precipitation aluminum hypophosphite added.

higher carbon residue. This is consistent with the TG analysis. This may be because that under the influence of heat, the AHP is decomposed and then generates aluminum pyrophosphate and aluminum phosphate which can form a stable carbon layer. The carbon layer will be denser with the incorporation of AHP. The hydrothermal AHP may be well dispersed in PUE with a small size; it can be more effective in promoting the process of composite materials turning into carbon due to its larger surface area. Furthermore, the carbon layer will cut off the heat radiation and oxygen, leading to a great improvement of the flame retardance of PUE/AHP composites.

In order to further evaluate the fire safety of the PUE/AHP composites, we introduce the fire performance index (FPI) defined as the proportion of the time to ignition (TTI) and PHRR value.¹⁶ When the FPI value increases, the fire risk of material is reduced. Comparing the FPI of PUE containing different types of AHP, it was found that hydrothermal AHP provides higher FPI, indicating lower fire risk of material.

Table III. Cone Calorimeter Data of PUE and PUE/AHP Composites

Sample	TTI ^a (s)	PHRR (KW·m ⁻²)	THR (MJ·m ⁻²)	FPI ^b	Mass loss (wt %)
PUE	130.5	618.7	35.3	0.211	80.4
AHPPUE1	99.4	159.2	21.2	0.624	57.5
AHPPUE2	89.4	117.9	17.7	0.758	45.2
AHPPUE3	81.7	100.6	13.6	0.812	35.1
AHPPUE4	101.3	189.2	25.0	0.535	59.1
AHPPUE5	94.3	126.1	18.7	0.747	47.7
AHPPUE6	90.5	115.5	13.3	0.784	44.7

^aTime to ignition.

^bFire performance index.

Table IV. LOI Data of PUE and PUE/AHP Composites

Sample	Content of AHP (wt %)	LOI (vol %)	Dripping
PUE	0	20.5	Y
AHPPUE1	1	22.7	Y
AHPPUE2	5	28.5	N
AHPPUE3	10	36.3	N
AHPPUE4	1	22.3	Y
AHPPUE5	5	28.1	N
AHPPUE6	10	35.2	N

Flammability of PUE/AHP Composites

The LOI is widely used to evaluate the flammability of polymer material, and the corresponding data are presented in Table IV. It can be seen that pure PUE is a flammable material with a low LOI value of 23.5 vol %. However, the LOI value of polyurethane elastomer increases to 28.5 vol % when 5 wt % hydrothermal AHP is added. Figure 9 shows the digital photos of the samples obtained from the LOI test, and it is easy to notice that PUE tends to drip during combustion. However, when 5 wt % AHP is added into the PUE matrix, dripping is inhibited to some extent. And dripping is completely suppressed with the addition of 10 wt % AHP. Obviously, pure PUE has little char residue left after combustion. However, all the PUE samples containing AHP have more char residue, and the residue increases with more AHP. According to these results, it can be concluded that the flame retardancy of PUE can be improved by the incorporation of AHP. Comparing the PUE containing the same amount of different types of AHP, we can find that PUE with the hydrothermal AHP added has higher LOI, which is consistent with the cone calorimetric analysis.

Mechanical Test of PUE/AHP Composites

The mechanical properties of PUE/AHP samples with different contents of AHP are shown in Table V. The incorporation of AHP affects the tensile strength of PUE. The values of the tensile strength and elongation at break are 23.65 MPa and 800% for pure PUE. With increasing AHP, these values further decrease. Comparing the data of AHPPUE1–3 and AHPPUE4–6, we can conclude that hydrothermal AHP has less effect on the tensile strength of PUE, still preserve excellent mechanical

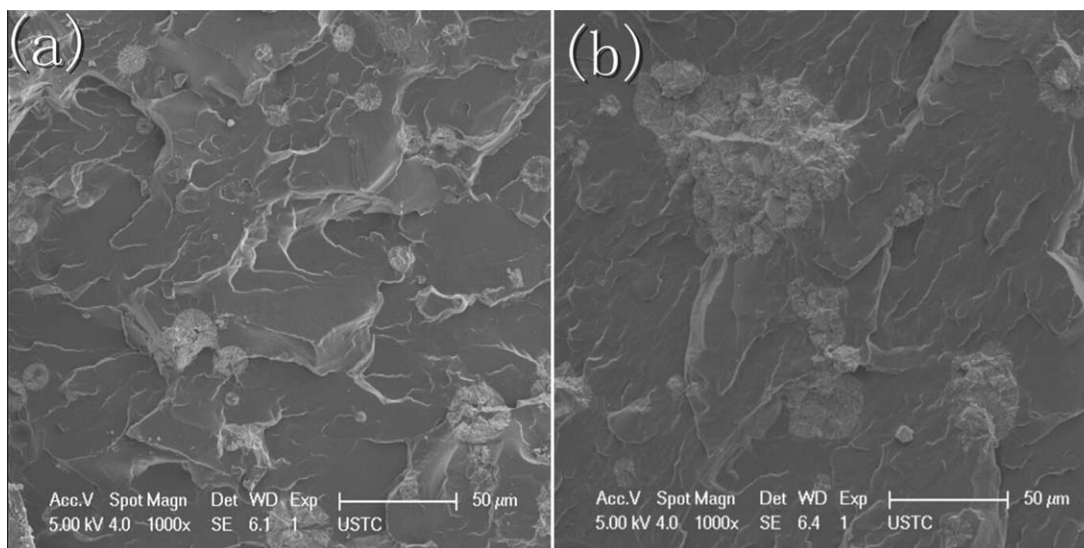


Figure 8. Section of PUE/AHP composites: (a) containing hydrothermal aluminum hypophosphite and (b) containing precipitation aluminum hypophosphite.

properties, which is mainly because that hydrothermal AHP has a more even dispersion in the matrix.

CONCLUSIONS

In this study, microsphere AHP was prepared via the hydrothermal method, and then both the hydrothermal AHP and the precipitation AHP were added to the PUE, respectively. The flame retardant properties, thermal stability, and mechanical properties of the PUE containing different types of AHP were investigated.

The results show that the hydrothermal AHP is spherical with a uniform particle size of around 5 μm . The two kinds of AHP have similar effects on the thermal stability of PUE, and the char residue at 600°C of the PUE with hydrothermal AHP added is higher than that of the PUE with precipitation AHP.

Compared with the PUE having precipitation AHP at the same amounts, the PUE containing hydrothermal AHP has lower PHRR and THR, higher LOI, and better flame retardance. This is mainly because that hydrothermal AHP can be well dispersed in PUE with a smaller size. And it can be more effective in promoting the process of composite materials changing into carbon due to its larger surface area. The carbon layer cuts off the heat radiation and oxygen, creating a great improvement in the flame retardance of PUE/AHP composites.

The incorporation of two kinds of AHP decreases the tensile strength of PUE, but the influence of hydrothermal AHP is smaller. It may be because that hydrothermal AHP can be well dispersed in PUE.

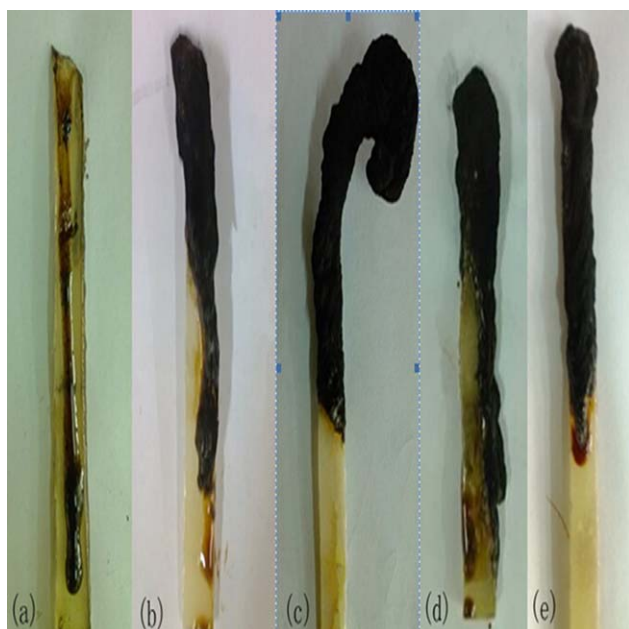


Figure 9. Digital photos of samples after LOI test: (a) AHPPUE, (b) AHP-PUE2, (c) AHPPUE3, (d) AHPPUE5, and (e) AHPPUE6. [Color figure can be viewed in the online issue, which is available at wileyonlinelibrary.com.]

Table V. Mechanical Properties of PUE and PUE/AHP Composites

Sample	Hardness (SHORE A)	Tensile strength (MPa)	Elongation at break (%)
PUE	63	23.65	806
AHPPUE1	66	22.75	767
AHPPUE2	73	20.05	718
AHPPUE3	78	19.58	672
AHPPUE4	67	22.50	746
AHPPUE5	75	19.88	682
AHPPUE6	80	18.38	639

ACKNOWLEDGMENTS

The authors thank the Research Fund for the Doctoral Program of Anhui Jianzhu University (2014) and National Key Technology R&D Program (2013BAJ01B05) for their financial support.

REFERENCES

1. Wang, Z. Y.; Liu, Y.; Wang, Q. J. *Polym. Degrad. Stab.* **2010**, *95*, 945.
2. Amina, L. M.; Mannal, A. E. S.; Ahmed, W. J. *Carbohydr. Polym.* **2014**, *102*, 724.
3. Cai, Y. Z.; Guo, Z. H.; Fang, Z. P.; Cao, Z. H. *J. Appl. Clay. Sci.* **2013**, *77–78*, 10.
4. Mohammad, Y.; Masoud, S. N.; Forszan, G.; Davood, G. *J. Inorg. Chim. Acta* **2011**, *371*, 1.
5. Wu, N. J.; Li, X. T. *J. Polym. Degrad. Stab.* **2014**, *105*, 268.
6. Xiao, S. S.; Chen, M. J.; Dong, L. P.; Deng, C.; Chen, L.; Wang, Y. Z. *J. Chin. J. Polym. Sci.* **2014**, *32*, 98.
7. Yang, L.; Han, X. Y.; Tang, X. J.; Han, C. X.; Zhou, Y. X.; Zhang, B. G. *J. Chin. Chem. Lett.* **2011**, *22*, 385.
8. Zhao, B.; Chen, L.; Long, J. W.; Chen, H. B.; Wang, Y. Z. *J. Ind. Eng. Chem. Res.* **2013**, *52*, 2875.
9. Yan, Y. W.; Huang, J. Q.; Guan, Y. H.; Shang, K.; Jian, R. K.; Wang, Y. Z. *J. Polym. Degrad. Stab.* **2014**, *99*, 35.
10. Yang, W.; Hu, Y.; Tai, Q. L.; Lu, H. D.; Song, L.; Richard, K. K. *J. Compos. Part A* **2011**, *42*, 794.
11. Yuan, B. H.; Bao, C. L.; Guo, Y. Q.; Song, L.; Kim, M. L.; Hu, Y. J. *Ind. Eng. Chem. Res.* **2012**, *51*, 14065.
12. Madkour, T. M.; Azzam, R. A. *Eur. Polym. J.* **2013**, *49*, 439.
13. Tang, G.; Wang, X.; Zhang, R.; Yang, W.; Hu, Y.; Song, L.; Gong, X. L. *J. Compos. Part A* **2013**, *54*, 1.
14. Wang, Z. T.; Zhang, X.; Bao, C.; Wang, Q. Y.; Qin, Y.; Tian, X. Y. *J. Appl. Polym. Sci.* **2012**, *124*, 3487.
15. Li, Q. F.; Li, B.; Zhang, S. Q.; Lin, M. J. *J. Appl. Polym. Sci.* **2012**, *125*, 1782.
16. Xiao, S. S.; Chen, M. J.; Dong, L. P.; Deng, C.; Chen, L.; Wang, Y. Z. *J. Chin. J. Polym. Sci.* **2014**, *32*, 98.